ELSEVIER

Chemometrics and Intelligent Laboratory Systems 32 (1996) 215–232

Chemometrics and intelligent laboratory systems

Second-order tensorial calibration for kinetic spectrophotometric determination

Yu-Long Xie [1], Juan José Baeza-Baeza, Guillermo Ramis-Ramos *

Department of Analytical Chemistry, University of Valencia, E-46100 Burjassot Valencia, Spain

Received 25 January 1995; accepted 18 September 1995

Abstract

Kinetic-diode array spectrophotometric detection, as well as other multichannel techniques when used in non-equilibrium conditions, constitute second-order instrumentation. The second-order response provided will be bilinear, under certain conditions even trilinear, thus allowing the use of the generalized rank annihilation method (GRAM) and the trilinear decomposition method (TLD). Both numerically simulated and experimental data were used to evaluate the performance of these calibration techniques. The conditions in which the 'second-order advantage' (the possibility of quantifying the analytes in the presence of unknown reactions or interferences) is preserved were investigated. The coupling reaction of diazotized sulfanilamide with *p*-, *o*- and *m*-amino benzoic acid, and with orciprenaline, to give azodyes was monitored. Binary mixtures of these substrates with different values of the rate constant ratio, and with various degrees of spectral overlap, were resolved. The advantages and limitations of higher-order data analysis techniques such as GRAM and TLD for the treatment of second-order kinetic data are discussed.

Keywords: Kinetic determinations; Generalized rank annihilation method; Trilinear decomposition method

1. Introduction

Modern analytical chemistry has benefited from the development of second- and higher-order instrumentation, that is, instruments capable of providing bi- and multi-dimensional data arrays, which usually results in a substantial improvement of the analytical capability [1]. In the last two decades, second-order instruments and techniques have become commonplace in analytical chemistry laboratories. Second-order instrumentation relies on two separated analytical mechanisms linked in series such that the signal of the latter is modulated by the former. A second-order tensor or a data matrix is generated for each single measurement run. This is the case for the so-called hyphenated techniques such as LC/UV-VIS, LC/MS, GC/MS, GC/FTIR, MS/MS and 2D-NMR [2,3], and other techniques such as two-dimensional excitation-emission fluorometry [2,3], multichannel detection spectroscopic titration [4] and flow optical sensors [5,6].

In a bilinear second-order device, that is, when the instrument response for a single analyte in an interference-free sample is a rank one matrix [7], calibration can be carried out using only one standard consisting of just the analyte, and the prediction will be

* Corresponding author.

[1] On leave from the Department of Chemistry, Xiangtan University, Xiangtan, People's Republic of China.

Elsevier Science B.V.
SSDI 0169-7439(95)00078-X

robust to the presence of uncalibrated interferences [8]. Thus, calibration and sample measurements can be performed in the presence of unknown components that are not included in the calibration model. This merit is usually called 'the second-order advantage' [9,10]. Several algorithms capable of exploiting 'the second-order advantage' using third-order data arrays provided by bilinear second-order instruments have been described [1]. The generalized rank annihilation method (GRAM) [11], parallel factor analysis (PARAFAC) [12] and trilinear decomposition (TLD) [13] are most widely used.

Rank annihilation factor analysis was originally developed by Ho et al. as an iterative procedure [14]. It was modified by Lorber to yield a direct solution of a standard eigenvalue problem [15,16]. Sanchez and Kowalski extended the method to the general case of several components that are not necessarily present in both the calibration and the unknown samples, obtained the solution by solving a generalized eigenproblem and called the method GRAM [11]. Algorithm modifications and theoretical studies of GRAM are still underway [17–22]. The applicability of GRAM has been demonstrated by the treatment of third-order data arrays generated by hyphenated chromatography [23,24], excitation-emission fluorescence [20,21] and flow optical sensors [5].

When a second-order instrument is used, calibration is performed at several standard concentrations and thus a third-order tensor is usually obtained. If a third-order data array follows a trilinear model [13], a unique decomposition can be obtained by direct trilinear decomposition (TLD). Actually, GRAM is a special case of TLD, where the third-order tensor consists of only two bilinear matrices. There are not many applications of TLD in the literature. Recently, Li et al. [25] and Booksh et al. [6] proposed modified algorithms for TLD.

When the signal of a first-order instrument is modulated by a chemical kinetic process, a second-order data array can be obtained, e.g. when a kinetic process is monitored by a diode-array UV/VIS detector. Recently, attention has been paid to the use of kinetic processes to increase the order of the data arrays. For the purpose of quantitative calibration, the linear and extended Kalman filter techniques have been applied to the treatment of multiwavelength kinetic data (second-order data) [26–28]. Also, multi-way principal component regression (PCR) [29] and multi-way partial least squares (PLS) [30,31] have been applied to quantitative calibration using second-order kinetic data. On the other hand, an attempt was made for the simultaneous qualitative and quantitative resolution of mixtures based on factor analysis of a second-order kinetic response from a single sample [32]. However, in the application of the mentioned methods the model should accurately describe the system behaviour for quantitative calibration and the qualitative resolution may not be unique owing to the rotational ambiguity of factor analysis.

The second-order response of a multiwavelength detection kinetic process would be bilinear, and under certain conditions a trilinear data array can be obtained from a series of calibration standards at increasing analyte concentrations. Thus, GRAM and TLD can be applied to obtain the unique resolution of the third-order kinetic data array. Qualitative kinetic and spectral profiles and quantitative concentration information of the analytes can thus be retrieved simultaneously in the presence of unknown co-existing interferences.

The aim of this work is to examine the applicability of high-order data analysis techniques such as GRAM and TLD to the kinetic analysis field, and to discuss the advantages and limitations of these approaches applied therein. As far as we know, the majority of research based on second-order response emphasized the use of the hyphenated chromatographic system. Although in the case of both the hyphenated chromatography and kinetic systems, coupled with a diode-array detector, the experiments involve the periodical acquisition of spectra for a single sample which changes over time, the nature of these changes are different. For the former case, no chemical reaction takes place and it is the molecular interaction of the solutes in the sample with both the mobile and the stationary phases that makes the amount of solute reaching the detector vary with time. The continuous nature of chromatographic peaks implies sequential appearance and disappearance of the concentration profiles of the solutes, which makes chemometric tools a useful supplement to separate incompletely resolved chromatograms of complex samples. For multicomponent kinetic systems, chemical reactions between the analytes and a common reagent take place, the amounts of spectrally active

species changing continuously with time following different reaction rates. In both cases, a wavelength–time second-order response matrix is acquired for each sample. However, kinetic curves present a rather monotonous variation of the signal with time starting from a point. This implies a stronger collinearity in the time order when compared to the sequential appearance and disappearance of peaks of the chromatographic profiles.

To our knowledge, there is no study in the literature concerning the treatment of second- or third-order kinetic data. In this paper, both numerically simulated and real experimental data were processed. The coupling reaction of diazotized sulfanilamide with the *o*-, *p*- and *m*-amino benzoic acids, and with orciprenaline, was used as a model system. Binary mixtures of these compounds with different ratios of the rate constants, and various degrees of spectral overlap of the coloured products, were measured to provide the second-order data arrays. The initial concentrations of the analytes in the presence of unknown interferences were determined together with their related kinetic curves and spectra.

2. Experimental

2.1. Apparatus

An HP 8452A diode array spectrophotometer (Hewlett-Packard, Palo Alto, CA, USA) provided with a 1 cm quartz cell was used in the kinetic measurements. The pH values of buffer solutions were adjusted with a Crison MicroPH 2001 pH meter provided with a combined glass electrode. A 500 μl piston pipette was used to inject a reagent to start the reactions. A 486 IBM compatible microcomputer was used to control the spectrophotometer and to acquire and treat the data. Data acquisition began 10 s after starting the reactions. The data files produced by the HP 89531A operation software (Hewlett-Packard) were processed by the authors' own programmes which were written in MATLAB (MathWorks, Sherborn, MA, USA).

2.2. Reagents and solutions

Reagent grade *o*-, *m*- and *p*-amino benzoic acid (ABA) (Merck, Darmstadt, Germany), orciprenaline (ORC) (kindly donated by Boehringer-Ingelheim, Barcelona, Spain), sulfanilamide (Sigma, St. Louis, MO, USA), sulfamic acid, sodium nitrite, sodium dodecyl sulphate (SDS) (Fluka, Buchs, Switzerland), and citric acid (Panreac, Barcelona, Spain) were used. Distilled demineralized water (Barnstead, Sybron, Taunton, MA, USA) was used throughout.

To buffer the solutions, citric acid and variable amounts of a sodium hydroxide solution were added. The final buffer concentration was 0.25 mol l^{-1} in all cases. The stock solutions of the substrates were prepared by dissolving 17.5 mg *o*-ABA, 17.5 mg *m*-ABA, 18.5 mg *p*-ABA and 56.3 mg ORC in 1 ml ethanol, and diluting with water to 50 ml. The 4×10^{-2} mol l^{-1} sulfanilamide stock solution was prepared in 0.3 mol l^{-1} HCl. The 0.2 mol l^{-1} $NaNO_2$, 0.5 mol l^{-1} sulfamic acid and 20% SDS solutions were made with water.

The 1×10^{-2} mol l^{-1} diazonium ion solution was prepared as follows: 12.5 ml sulfanilamide was introduced into a 50 ml volumetric flask, and 15 ml $NaNO_2$ was added. The mixture was allowed to react for 10 min, then 15 ml sulfamic acid was added to destroy the excess nitrite, and after another 15 min the solution was made up to the mark with water. The diazonium ion solution was renewed daily.

2.3. Optimization of the reaction conditions

To test the method the coupling reaction of diazotized sulfanilamide with *o*-, *m*- and *p*-amino benzoic acid (ABA), and with orciprenaline (ORC), to give coloured azodyes was used. Since only the basic form of the ABAs (the non-ionic free amines) is sufficiently activated to couple with diazonium ions, the reaction rate is strongly affected by pH [33]. We have found that, at pH lower than 3.5, the reactions were too slow, and at pH higher than 5.5, some of the analytes coupled in less than 1 min, which was not suitable for the manual mixing procedure used. On the other hand, at pH values higher than 5.5, the absorbance of the reagent blank was large. This has been shown to be due to hydrolysis of the diazonium ion to yield a phenol which couples with the excess reagent [34]. In addition, at higher pH values, the azo dyes were unstable, and the absorbance decreased rapidly after reaching a maximum value. For the convenience of manual operation, a compromise

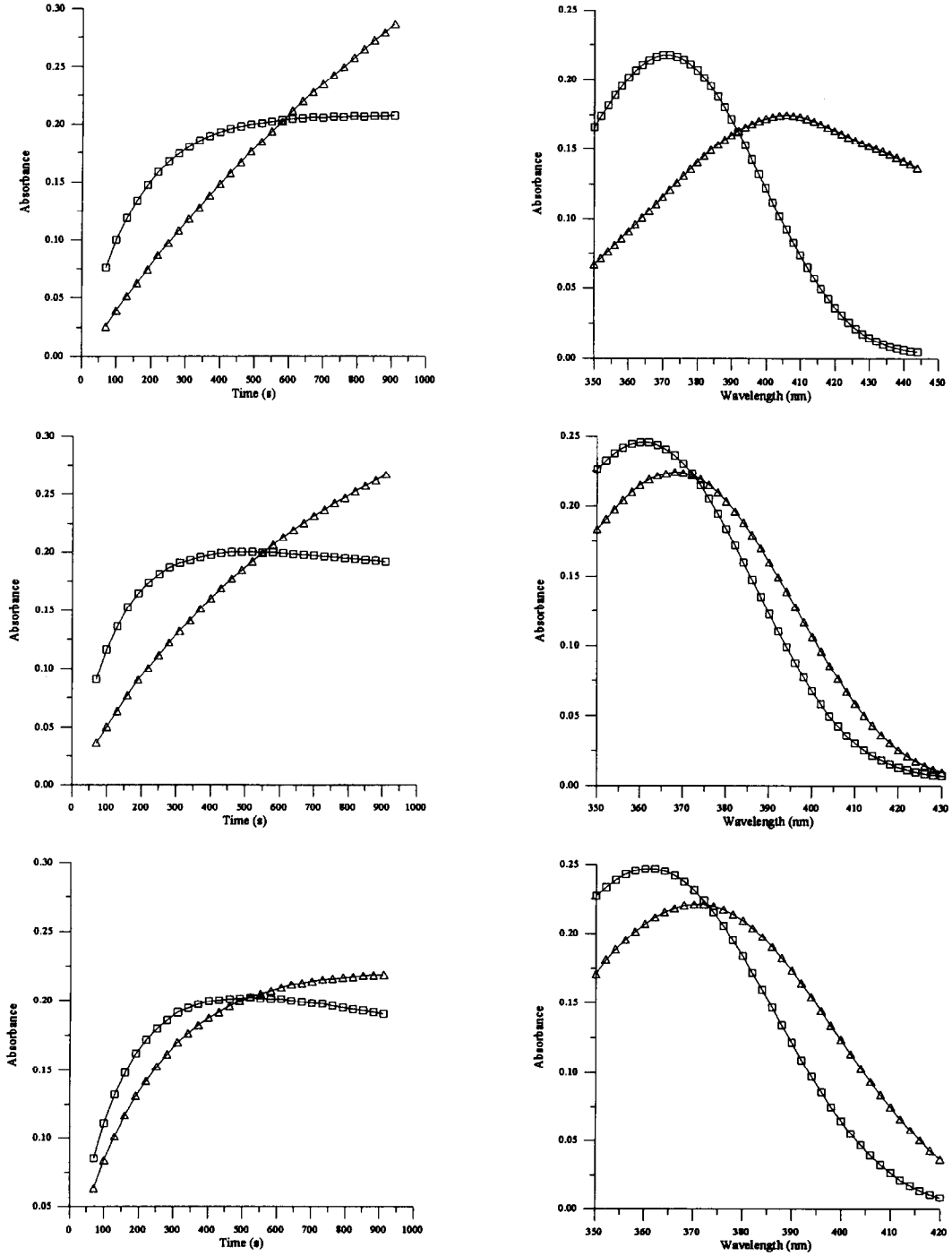

Fig. 1. Kinetic curves (left) and spectra (right) for the following binary mixtures: upper part, ORC (△) and *o*-ABA (□); middle part, *p*-ABA (△) and *m*-ABA (□); lower part, *o*-ABA (△) and *m*-ABA (□).

should be made between suitable reaction rate and avoidance of hydrolysis of the diazonium ion. Three pH values within these two extremes, i.e. 3.80, 3.90 and 4.10 as indicated in Table 1, were adopted for carrying out the experiments. Furthermore, it was observed that the addition of sodium dodecyl sulphate (SDS) can stabilize the azo dyes, therefore a final concentration of 2% SDS was used.

Three binary combinations of substrates, i.e. *o*-ABA/ORC, *m*-ABA/*p*-ABA and *o*-ABA/*m*-ABA, were used to observe the kinetic process under the conditions given in Table 1 and to provide experimental data. Under the adopted conditions, the substrates in each binary combination possessed different values of the rate constant ratio and the product spectra overlapped seriously. The kinetic curves and the spectra of the azodyes are shown in Fig. 1. The monitored wavelength regions were from 350 to 444 nm for *o*-ABA/ORC, from 350 to 430 nm for *m*-ABA/*p*-ABA and from 350 to 420 nm for *o*-ABA/*m*-ABA. At the monitored wavelengths the analytes do not absorb, and the diazotized sulfanilamide has a very low molar absorptivity. Further, the absorbance due to the diazonium ion is maintained at an almost constant value owing to the large reagent concentration in relation to the analyte concentrations. For this reason, each binary system contained only two significant spectrally active species.

Table 1 also lists the rate constants of the substrates which were evaluated with a series of three single component solutions (Nos. 14 to 19 in Table 2) assuming that first order was followed. The Powell algorithm was used to compute the rate constants. The occurrence of hydrolysis of the product which is observed for *m*-ABA in Fig. 1 was neglected in the computation of rate constants.

Table 1
First-order rate constants for *o*-, *m*-, and *p*-ABA, and ORC at different pH values in a 2% SDS medium [a]

Binary mixture	Substrate	λ_{max} (nm)	pH	$k \pm s_k$ ($s^{-1} \times 10^{-3}$) [b]
I	*o*-ABA	370	4.10	6.31 ± 0.12
	ORC	406	4.10	1.20 ± 0.03
II	*m*-ABA	360	3.90	8.16 ± 0.40
	p-ABA	368	3.90	1.67 ± 0.11
III	*o*-ABA	370	3.80	4.48 ± 0.08
	m-ABA	360	3.80	7.14 ± 0.07

[a] ABA, amino benzoic acid; ORC, orciprenaline.
[b] Obtained from three single component solutions with increasing substrate concentrations (concentrations given in Table 2, experiments Nos. 14 to 19).

Table 2
Composition of the binary mixtures

Experiment No. [a]	*o*-ABA/ORC ($\times 10^{-5}$ mol l^{-1})	*m*-ABA/*p*-ABA ($\times 10^{-5}$ mol l^{-1})	*o*-ABA/*m*-ABA ($\times 10^{-5}$ mol l^{-1})
1	2.759/3.456	1.839/1.945	2.299/2.299
2	4.139/3.456	3.219/1.945	2.299/3.679
3	5.518/3.456	4.598/1.945	2.299/5.058
4	2.759/5.184	1.839/3.403	3.679/2.299
5	4.139/5.184	3.219/3.403	3.679/3.679
6	5.518/5.184	4.598/3.403	3.679/5.058
7	2.759/6.912	1.839/4.861	5.058/2.299
8	4.139/6.912	3.219/4.861	5.058/3.679
9	5.518/6.912	4.598/4.861	5.058/5.058
10	3.679/4.320	2.759/3.889	3.219/2.759
11	3.679/6.048	3.679/2.917	4.139/4.599
12	4.599/4.320	2.299/3.403	4.139/2.759
13	4.599/6.048	3.219/2.431	3.219/4.599
14	2.759/0.000	1.839/0.000	2.299/0.000
15	4.139/0.000	3.219/0.000	3.679/0.000
16	5.518/0.000	4.598/0.000	5.058/0.000
17	0.000/3.456	0.000/1.945	0.000/2.299
18	0.000/5.184	0.000/3.403	0.000/3.679
19	0.000/6.912	0.000/4.861	0.000/5.058

[a] Each mixture from Nos. 14 to 19 was used once as the calibration sample to resolve mixtures from Nos. 1 to 13 with GRAM; either mixtures from Nos. 14 to 16 and from Nos. 17 to 19 were used as calibration samples to resolve mixtures from Nos. 1 to 13 and mixtures from Nos. 1 to 9 were used as the calibration samples to resolve mixtures from Nos. 10 to 13 with TLD. The errors of the estimated concentrations are given in Tables12–14.

2.4. Procedure used to obtain the experimental data

For each binary combination, the series of single and mixed solutions of Table 2 were prepared by introducing aliquots of the corresponding stock solutions, 20 ml buffer solution and 2.5 ml SDS into a 25 ml volumetric flask, and the volume was completed with water. A 2.25 ml volume was transferred into a dry 1 cm quartz cell, the reaction was started by injecting 0.25 ml diazonium ion solution, and a keyboard button was simultaneously pressed to start the data acquisition period ($t = 0$). Mixing was facilitated by bubbling the solution in the cell four times with the piston pipette. The spectra were scanned ev-

ery 30 s, from $t = 10$ s to $t = 910$ s. Each spectrum was acquired in the monitored wavelength region mentioned above with a 2 nm resolution. The blank was prepared in the same way in the absence of the substrate. The blank absorbance matrix was always subtracted from the sample absorbance matrices before processing the data. For each solution of the *o*-ABA/ORC, *m*-ABA/*p*-ABA and *o*-ABA/*m*-ABA binary mixtures, a 48×31, 41×31 and 36×31 wavelength–time data matrix was obtained, respectively. Owing to the perturbations and noise, the spectra corresponding to the first two time points were rejected in the computation. Finally, the initial concentrations of the analytes were estimated using GRAM and TLD, and the retrieved kinetic curves and spectra were compared with those measured experimentally.

3. Kinetic data structure

3.1. Nomenclature

Lowercase bold characters are used for column vectors, uppercase bold characters for second-order tensors (or two-way matrices), and underlined italic uppercase bold characters for third-order tensors (or three-way matrices). The transpose of a matrix or a vector is represented by the superscript T and the inverse of a matrix is signified by the superscript '-1'. Unless otherwise stated, lowercase and uppercase plain characters are used for scalars and as running indices, and also to indicate the number of the dimensions of the vectors and matrices.

3.2. Bilinearity and trilinearity consideration in chemical kinetics

Let us suppose a mixture contains L active substrates, C_l ($l = 1,...,L$), which couple with a common reagent, R, following a first- or pseudo-first order reaction:

$$C_l + R \rightarrow P_l \tag{1}$$

Assuming that the change of absorbance is due only to the change in the concentration of the products, i.e. the reactants are all taken as transparent at the monitored wavelengths, and that the absorbances are additive and follow the Lambert–Beer law, we can write the response of a kinetic reaction monitored with a diode-array detector as:

$$A_{i,j} = \sum_{l=1}^{L} (1 - e^{-k_l t_i}) c_l s_{j,l} \tag{2}$$

where $A_{i,j}$ is the change of absorbance of the mixture at time t_i ($i = 1,...,I$), and at wavelength λ_j ($j = 1,...,J$) with respect to the change observed at the same time and wavelength values for the blank solution, k_l is the rate constant corresponding to species C_l ($l = 1,...,L$), $s_{j,l}$ is the sensitivity (the molar absorptivity multiplied by the optical pathlength) of product P_l at λ_j, and c_l is the initial concentration of species C_l. For a deduction of Eq. (2), see, e.g., Connors [35]. Eq. (2) can be rewritten as:

$$\mathbf{A} = \sum_{l=1}^{L} \mathbf{k}_l c_l \mathbf{s}_l^{\mathrm{T}} = \mathbf{K}\mathbf{C}\mathbf{S}^{\mathrm{T}} \tag{3}$$

where $\mathbf{A}$ is an $I \times J$ matrix containing the wavelength–time information of the kinetic system, $\mathbf{k}_l$ is a vector containing the kinetic information for the lth component whose generic element is $[1 - \exp(-k_l t_i)]$, and $\mathbf{s}_l$ is the sensitivity vector of product P_l. Thus, $\mathbf{K}$ ($= \{\mathbf{k}_l\}$) is an $I \times L$ matrix which contains the kinetic information of the analytes (one domain of the second-order instrument), $\mathbf{S}$ ($= \{\mathbf{s}_l\}$) is a $J \times L$ matrix containing the spectral information of the absorbing products of the analytes (another domain of the second-order instrument), and $\mathbf{C}$ is a diagonal matrix with the concentration of the analytes as its diagonal elements.

In the chemometric literature, for a second-order device, if the rank of the response of a sample containing only a pure analyte is one, then the second-order device and the data matrix obtained are both called bilinear. In this sense, the second-order kinetic response matrix expressed as in Eq. (3) and the data matrices obtained under the adopted experimental conditions can be regarded as bilinear. However, the rank of a reaction system is not always trivial [36].

Usually, to construct a prediction model, several (say N) samples of known composition and different concentrations of the substrates should be measured,

and then N $I \times J$ bilinear matrices would be obtained:

$$\mathbf{A}_1 = \mathbf{K}\mathbf{C}_1\mathbf{S}^T \quad (4a)$$

$$\mathbf{A}_2 = \mathbf{K}\mathbf{C}_2\mathbf{S}^T \quad (4b)$$

$$\mathbf{A}_N = \mathbf{K}\mathbf{C}_N\mathbf{S}^T \quad (4n)$$

Under the assumption of first or pseudo-first reaction mechanism, **K** and **S** in the bilinear matrices of Eq. (4) will be the same for the N samples with different concentration ratio of the substrates. Stacking these N bilinear matrices into a $N \times I \times J$ three-way data array, the following trilinear model is obtained:

$$A_{n,i,j} = \sum_{l=1}^{L} (1 - e^{-k_l t_i}) c_{n,l} s_{j,l} \quad (5)$$

or:

$$\underline{A} = \sum_{l=1}^{L} \mathbf{k}_l \otimes \mathbf{c}_l \otimes \mathbf{s}_l \quad (6)$$

where $\underline{A}$ is an $N \times I \times J$ third-order response tensor with generic element $A_{n,i,j}$, and $\mathbf{c}_l$ is the concentration vector of the lth analyte in the N samples, and the symbol $\otimes$ represents the tensor product (outer product) [37].

It is our purpose to determine the initial concentrations of the reactants and their related kinetic curves and spectra based upon the third-order tensor $\underline{A}$ without explicit knowledge about the kinetic system.

Eqs. (3) and (6) are derived with the requirement that the kinetic reaction follows the first-order mechanism of Eq. (1). However, in some other instances and so far as the Lambert–Beer and additivity laws are followed, similar expressions would also be obtained. For example, if the products are not stable and are hydrolysed following a parasitic first- or pseudo-first order law:

$$C_l + R \rightarrow P_l \quad (7a)$$

$$P_l \rightarrow D_l \quad (7b)$$

a response model similar to Eq. (2) can be derived [35]:

$$A_{i,j} = \sum_{l=1}^{L} \frac{k_l}{k'_l - k_l} (e^{-k_l t_i} - e^{-k'_l t_i}) c_l s_{j,l} \quad (8)$$

where k_l and k'_l represent the first-order rate constants for the formation and hydrolysis of the P_l products, respectively, and where we have also assumed that the D_l final products do not absorb. In both these response models defined by Eqs. (2) and (8), the kinetic behaviour, the spectral response and the concentrations are independent from one another, and thus the general bilinear and trilinear models expressed by Eqs. (3) and (6) are also valid.

Let us now consider a more complex case in which some components of the mixture react with a common reagent R following a second-order law. The response model is [35]:

$$A_{i,j} = \sum_{l=1}^{L} \left[1 + \frac{1}{k_l c_l t_i}\right]^{-1} c_l s_{j,l} \quad (9)$$

where k_l is the second-order rate constant of the analyte C_l, and where the same presumption that only the products absorb is assumed.

According to Eq. (9), the response of a single standard is a rank one matrix, but the trilinear response model of Eq. (6) cannot be derived because the time-dependent kinetic profile is also dependent upon the initial concentration of the reactants. Thus, the kinetic profile for each substrate will be different for the sample with varied concentrations of the substrate, i.e. the bilinear matrices from different samples will have different bases. However, if we assume that only the unknown interferences follow the second-order law of Eq. (9), and that the species of interest follow the model of Eqs. (2) or (8) or any other linear response–concentration relationship, calibration with the GRAM and TLD methods by using the generalized standard addition method with a fixed background will be still possible [38]. The contribution of the second-order component to the response will be the same for all the data matrices obtained before and after the standard additions, and the overall response will still follow the trilinear model of Eq. (6). Obviously, the meaning of **k** for the interferences will be different from that of the analytes.

4. Algorithm of GRAM and TLD

The algorithms of GRAM and TLD have been documented extensively elsewhere

[5,6,11,13,18,21,25]. Here the algorithm of Wilson et al. [18] for GRAM, and the modified algorithm of Booksh et al. [6] for TLD have been adopted, and only a brief presentation is given below.

In the GRAM, a bilinear matrix, **N**, obtained with a single standard is used for calibration, and the analyte concentrations in an unknown sample are estimated through its corresponding bilinear matrices **M** together with **N**. GRAM solves the generalized eigenproblem:

$$\mathbf{M}\Psi = \mathbf{N}\Psi\Lambda \tag{10}$$

$$\Lambda = \mathbf{C_M} \cdot \mathbf{C_N^{-1}} \tag{11}$$

where Ψ and Λ are matrices of eigenvectors and eigenvalues, and $\mathbf{C_M}$ and $\mathbf{C_N}$ are diagonal matrices whose diagonal elements are the concentrations of the analytes in the corresponding sample.

The QZ algorithm [39] can be used to solve the generalized eigenproblem. However, to apply the QZ algorithm **N** and **M** should be square matrices, and thus it is necessary to transfer the usual rectangular **N** and **M** matrices into square matrices. To accomplish such transformation, **N** and **M** must be projected into a common base set. According to Wilson et al. [18], two sets of orthonormal vectors $\mathbf{P}\,(=\{\mathbf{p}_i\})$ and $\mathbf{Q}\,(=\{\mathbf{q}_i\})$ that are base sets of the joint column and row spaces, respectively, of **N** and **M** were determined from the adjoint matrices (**M**|**N**) and (**M**/**N**) by the use of singular value decomposition (SVD):

$$(\mathbf{M}|\mathbf{N}) = \mathbf{P} \cdot \mathbf{S_1} \cdot \mathbf{V}^{\mathrm{T}} \tag{12}$$

$$\left(\frac{\mathbf{M}}{\mathbf{N}}\right) = \mathbf{U} \cdot \mathbf{S_2} \cdot \mathbf{Q}^{\mathrm{T}} \tag{13}$$

where **P**, **V**, **U**, and **Q** are singular vectors (eigenvectors), and $\mathbf{S_1}$ and $\mathbf{S_2}$ are matrices of singular values. Once **P** and **Q** are determined, **M** and **N** are projected into a common base set:

$$\mathbf{M_{PQ}} = \mathbf{P}^{\mathrm{T}} \cdot \mathbf{M} \cdot \mathbf{Q} \tag{14}$$

$$\mathbf{N_{PQ}} = \mathbf{P}^{\mathrm{T}} \cdot \mathbf{N} \cdot \mathbf{Q} \tag{15}$$

Then, the eigenproblem in Eq. (10) can be solved via the QZ algorithm where $\mathbf{M_{PQ}}$ and $\mathbf{N_{PQ}}$ are substituted by **M** and **N**:

$$\mathbf{M_{PQ}} \cdot \Psi = \mathbf{N_{PQ}} \cdot \Psi \cdot \Lambda \tag{16}$$

The estimate of the concentration in an unknown sample, $\mathbf{C_M}$, can be obtained from the eigenvalue matrix Λ and the concentration of the calibration sample $\mathbf{C_N}$. The estimated response matrices in both orders, **X** and **Y** (in kinetic analysis, they are **K** and **S** as expressed in Eq. (3)), can be calculated according to the equations given below:

$$\mathbf{X} = \mathbf{P} \cdot (\mathbf{N_{PQ}} + \mathbf{M_{PQ}}) \cdot \Psi \tag{17}$$

$$\mathbf{Y} = \mathbf{Q} \cdot (\Psi^{-1})^{\mathrm{T}} \tag{18}$$

TLD can be viewed as an extension of GRAM where multiple standards (say N) rather than a single standard are used. It is necessary to find two matrices that are representative of all the bilinear matrices and that meet the necessary condition to apply the GRAM. With the application of a Tucker-3 model, Sanchez and Kowalski [13] constructed two pseudosamples that are linear combinations of the N bilinear response matrices, $\mathbf{A}_1$ to $\mathbf{A}_N$, of the N samples projected into a common row and column spaces. The steps to be followed are indicated next.

The third-order tensor $\underline{A}$ in Eq. (6) is rearranged into three adjoint matrices $\{\mathbf{A}_n\}$, $\{\mathbf{A}_i\}$ and $\{\mathbf{A}_j\}$, where $\mathbf{A}_n$ are $I \times J$ slices of $\underline{A}$, $\mathbf{A}_i$ are $J \times N$ slices of $\underline{A}$ and $\mathbf{A}_j$ are $N \times I$ slices of $\underline{A}$. The adjoint row, column and tube spaces of the third-order tensor $\underline{A}$ can be determined by SVD:

$$[\mathbf{A}_1|\mathbf{A}_2|\mathbf{A}_3|\ldots|\mathbf{A}_N] = \mathbf{U_r} \cdot \mathbf{S_r} \cdot \mathbf{V_r^T};\ \mathbf{U} = \mathbf{U_r}(I \times L) \tag{19a}$$

$$[\mathbf{A}_1|\mathbf{A}_2|\mathbf{A}_3|\ldots|\mathbf{A}_I] = \mathbf{U_c} \cdot \mathbf{S_c} \cdot \mathbf{V_c^T};\ \mathbf{V} = \mathbf{U_c}(J \times L) \tag{19b}$$

$$[\mathbf{A}_1|\mathbf{A}_2|\mathbf{A}_3|\ldots|\mathbf{A}_J] = \mathbf{U_t} \cdot \mathbf{S_t} \cdot \mathbf{V_t^T};\ \mathbf{W} = \mathbf{U_t}(N \times 2) \tag{19c}$$

where L is the number of principal components retained to reconstruct the model. Ideally, L equals the number of intrinsic physical factors, i.e. the number of analytes.

When **U**, **V** and **W** have been determined, the third-order tensor $\underline{A}$ is projected down to the (**U**, **V**, **W**) base sets, and the projected tensor $\underline{G}$ which consists of two $L \times L$ matrices, $\mathbf{G}_1$ and $\mathbf{G}_2$, is obtained:

$$\mathbf{G_1} = \sum_{n=1}^{N} w_{n2}(\mathbf{U}^{\mathrm{T}} \cdot \mathbf{A}_n \cdot \mathbf{V}) \tag{20a}$$

$$\mathbf{G_2} = \sum_{n=1}^{N} w_{n1}(\mathbf{U}^{\mathrm{T}} \cdot \mathbf{A}_n \cdot \mathbf{V}) \tag{20b}$$

where $\mathbf{G}_1$ and $\mathbf{G}_2$ are $L \times L$ full rank square matrices. The next step is to solve the simultaneous eigenproblem of the two matrices $\mathbf{G}_1$ and $\mathbf{G}_2$:

$$\mathbf{G}_1\mathbf{\Psi}_a = \mathbf{G}_2\mathbf{\Psi}_a\mathbf{\Lambda}_a \quad (21a)$$

$$\mathbf{G}_1^{\mathrm{T}}\mathbf{\Psi}_b = \mathbf{G}_2^{\mathrm{T}}\mathbf{\Psi}_b\mathbf{\Lambda}_b \quad (21b)$$

Here the $\mathbf{\Psi}$ and $\mathbf{\Lambda}$ symbols are the eigenvectors and eigenvalues of the corresponding eigenproblems as calculated by the QZ algorithm. According to Booksh et al. [6], it is better to use only one of the solutions of Eqs. (21a) and (21b) to estimate the intrinsic physical profiles, $\mathbf{X}$ and $\mathbf{Y}$:

$$\mathbf{Y} = \mathbf{V} \cdot \left(\mathbf{\Psi}_a^{\mathrm{T}}\right)^{-1} \quad \mathbf{X} = \mathbf{U} \cdot \mathbf{G}_2 \cdot \mathbf{\Psi}_a \quad (22a)$$

$$\mathbf{Y} = \mathbf{V} \cdot \mathbf{G}_2^{\mathrm{T}} \cdot \mathbf{\Psi}_b \quad \mathbf{X} = \mathbf{U} \cdot \left(\mathbf{\Psi}_b^{\mathrm{T}}\right)^{-1} \quad (22b)$$

The calculation of $\mathbf{X}$ and $\mathbf{Y}$ from the same eigenproblem is said to be able to provide reliable calibration results when imaginary eigenvectors are included in the solution of the eigenproblem and avoiding the occurrence of mismatched eigenvectors. The use of Eq. (22a) or Eq. (22b) depends on the value of the condition number of $\mathbf{\Psi}_a$ and $\mathbf{\Psi}_b$. The $N \times L$ matrix of the relative concentration ratios, $\mathbf{C}$, can be estimated by a least squares procedure when $\mathbf{X}$ and $\mathbf{Y}$ have been computed:

$$\mathbf{C} = \mathbf{P} \cdot \mathbf{Q}^{-1} \quad (23)$$

where

$$P_{n,l} = \sum_{i=1} \sum_{j=1} A_{n,i,j} \cdot X_{n,i} \cdot Y_{n,j} \quad (24)$$

and

$$Q_{s,t} = \sum_{i=1}^{I} \left(X_{i,s} \cdot X_{i,t}\right) \sum_{j=1}^{J} \left(Y_{j,s} \cdot Y_{j,t}\right) \quad (s,t = 1,\ldots,L) \quad (25)$$

5. Simulation

5.1. Mixtures of components following independent first-order reactions

The spectra of the components were generated as Gaussian peaks, and the curves were constructed following the first-order kinetic law. The response tensors of the mixtures were synthesized according to Eqs. (2) and (5).

Table 3
Parameters used in the simulation of the data sets for mixtures of four components that follow first-order reactions in the absence of noise [a]

Width of peaks (σ):	20 arbitrary units			
Wavelength range:	1 to 100 with intervals of 1			
Time range:	10 to 1210 s with 30 s intervals			
Variation of spectral overlap (peak positions in arbitrary units)				
Species	1	2	3	4
	38	**46**	**54**	**62**
	41	**47**	**53**	**59**
	44	**48**	**52**	**56**
	47	**49**	**51**	**53**
	48	**49**	**50**	**51**
Variation of kinetic overlap (rate constants in $s^{-1} \times 10^{-3}$)				
Species	1	2	3	4
	4.00	**8.00**	**12.0**	**16.0**
	4.00	**6.00**	**8.00**	**10.0**
	4.00	**5.00**	**6.00**	**7.00**
	4.00	**4.50**	**5.00**	**5.50**
	4.00	**4.25**	**4.50**	**4.75**
	4.00	**4.10**	**4.20**	**4.30**

[a] The errors of the estimated concentrations were negligible (see text).

Up to four-component mixtures were generated for the noise-free case. The parameters used in the simulation are listed in Table 3. The width of the spectral peaks were fixed to a constant value of $s = 20$ arbitrary units ($2s$ = distance between the inflection points), and the number of points, which were evenly spaced along the spectral order, was 100. The distances among peaks were shortened to increase the spectral overlap, and at the same time, the difference of the first-order kinetic rate constants among the components was reduced. A total of 30 different combinations of kinetic and spectral parameters was used in the simulation. The kinetic process was assumed to be monitored in the 10–1210 s time range with 30 s intervals. Thus a 100×41 data matrix was obtained for each mixture. The response of several mixtures and solutions of the isolated components, with increasing concentrations of the components, were generated for each combination of spectral and kinetic parameters.

To obtain the simulated experiments, normally distributed random numbers were generated and added to the calculated data of the theoretical re-

sponse matrix of each assumed mixture. The standard deviation of the noise was a percentage of the maximum absorbance value in the corresponding data matrix. First, two series of two-component mixtures that followed the model of Eqs. (2) and (5) were assumed. The parameters used for this simulation are summarized in Table 4. In one of the series, the spectral and kinetic parameters used in the simulation were fixed and only the standard deviation of the noise was changed. In the other series, the noise standard deviation was fixed and the spectral and kinetic overlap were increased simultaneously by shortening the distance between the peaks and by approaching the rate constant ratio of the two compo-

Table 4
Parameters used in the simulation of data sets for mixtures of two components that follow first-order reactions. Study of the influence of noise and overlap

Series I:					
Width of peaks (σ):	20 arbitrary units				
Wavelength range:	1 to 100 with intervals of 1 arbitrary unit				
Position of peaks:	30 and 60 for species 1 and 2, respectively				
Rate constants:	3×10^{-3} and 6×10^{-3} s^{-1} for species 1 and 2, respectively				
Time range:	10 to 1210 s with 30 s intervals				
Variation of noise level					
Case No.	1	2	3	4	5
Noise standard deviation [a]:	**0.0050**	**0.010**	**0.030**	**0.050**	**0.10**
Series II:					
Width of peaks (σ):	20 arbitrary units				
Wavelength range:	1 to 100 with intervals of 1 arbitrary unit				
Variation of spectral and kinetic overlap					
Case No.	6	7	8	9	10
Position of peaks:	**40/60**	**42/58**	**44/56**	**46/54**	**48/52**
Rate constants ($\times 10^{-4}$ s^{-1}):	**30/60**	**33/57**	**36/54**	**39/51**	**42/48**
Time range:	10 to 1210 s with 60 s intervals				
Noise standard deviation [a]:	0.030				
Composition of solutions (relative concentration)					
No.	Species 1		Species 2		
1	1		1		
2	2		1		
3	3		1		
4	1		2		
5	2		2		
6	3		2		
7	1		3		
8	2		3		
9	3		3		
10 [b]	**1.5**		**1.3**		
11	1		0		
12	2		0		
13	3		0		
14	0		1		
15	0		2		
16	0		3		

[a] The noise standard deviation is the value given multiplied by the maximum absorbance value in each data matrix. In these experiments the noise ranged from 0.5 to 10%.
[b] Mixture No. 10 was used as the unknown sample. The errors of the estimated concentrations are given in Table 8.

nents to unity. Ten two-component mixtures and three solutions of the individual components with different concentrations were assumed. The solutions of the pure components were used as the calibration samples for the GRAM. Both the three pure solutions and the first nine mixtures were used as the multiple calibration samples with TLD. Mixture No. 10 was regarded as the unknown sample, and each component was sequentially considered as the analyte.

The simulated response for another set of 13 three-component mixtures was obtained by assuming that the three components obeyed the first-order law.

Table 5
Parameters used in the simulation of the data sets for mixtures of three components that follow first-order reactions

Width of peaks (σ):	20 arbitrary units
Wavelength range:	1 to 100 with intervals of 1 arbitrary unit
Position of peaks:	35/50/65 for species 1/2/3, respectively
Rate constants: ($\times 10^{-4}$ s^{-1})	30/60/90 for species 1/2/3, respectively
Time range:	10 to 1210 s with 30 s intervals
Noise standard deviation [a]:	0.030

Composition of solutions (relative concentration)

No.	Species 1	Species 2	Species 3
1	1	1	1
2	2	1	2
3	3	1	3
4	1	2	2
5	2	2	3
6	3	2	1
7	1	3	3
8	2	3	1
9	3	3	2
10	1.5	1.3	1.2
11	1.5	1.3	1.4
12	2.5	2.4	1.6
13	2.5	2.4	1.8
14	1	0	0
15	2	0	0
16	3	0	0
17	0	1	0
18	0	2	0
19	0	3	0
20	0	0	1
21	0	0	2
22	0	0	3

[a] The noise standard deviation is the value given multiplied by the maximum absorbance value in each data matrix. The errors of the estimated concentrations are given in Table 9.

Table 6
Parameters used in the simulation of the data set for mixtures of two components when one of them undergoes a first-order reaction and the other one two consecutive first-order reactions

Width of peaks (σ):	20 arbitrary units
Wavelength range:	1 to 100 with intervals of 1 arbitrary unit
Position of peaks:	40/60 for species 1/2, respectively
Rate constants [a]:	species 1: $k_1 = 4\times10^{-3}$ s^{-1}
	species 2: $k_2 = 4\times10^{-3}$ s^{-1} and $k'_2 = 1.4\times10^{-3}$ s^{-1}
Time range:	10 to 1210 s with 30 s interval
Noise standard deviation [b]:	0.030

Composition of solutions (relative concentration)

No.	Species 1	Species 2
1	1	1
2	2	1
3	3	1
4	1	2
5	2	2
6	3	2
7	1	3
8	2	3
9	3	3
10	1.5	1.3
11	1.5	1.3
12	2.5	2.4
13	2.5	2.4
14	1	0
15	2	0
16	3	0
17	0	1
18	0	2
19	0	3

[a] For component 2, k_2 and k'_2 are the first-order rate constants of product formation and hydrolysis of the product, respectively.
[b] The noise standard deviation is the value given multiplied by the maximum absorbance value in each data matrix. The errors of the estimated concentrations are given in Table 10.

The response was constructed by Eqs. (2) and (5). The parameters used in the simulation are shown in Table 5. Similarly to the two-component situation of above, each pure solution was used as the calibration sample for GRAM, and both the three pure solutions and the first nine mixtures were used as multiple calibration samples for TLD. Once again, each component was taken as the analyte and the other two were regarded as unknown interferences. Here, all the 13 mixtures were used as the unknown samples for GRAM and for TLD when the three pure solutions were used as the calibration samples, and the four

mixtures from No. 10 to No. 13 were considered as the unknown samples for TLD while the first nine mixtures were used as the calibration samples.

5.2. Mixture of two components when one of them undergoes a first-order reaction and the other follows two consecutive first-order reactions

A mixture of two components in which one component followed the first-order law of Eq. (1) and the other followed the reaction process described by Eq. (7) was assumed. The response was constructed according to Eqs. (2) and (8), respectively. The parameters used in this simulation are listed in Table 6. Similarly, the response of a set of mixtures and several pure solutions of each component were simulated, and used as the calibration and prediction samples for GRAM and TLD. Both components were regarded as the analyte alternatively.

5.3. Mixtures with both first-order and second-order reactions

The responses for two-component and three-component systems were generated. In each case, one of

Table 7
Parameters used in the simulation of the data sets for mixtures of components that undergo first-order reactions in the presence of a second-order reaction

Series I:			
Width of peaks (σ):		20 arbitrary units	
Wavelength range:		1 to 100 with intervals of 1 arbitrary unit	
Position of peaks:		40/60 for species 1/2, respectively	
Rate constants:		$k_1 = 4 \times 10^{-3}$ s^{-1}	
		$k_2 = 0.15$ s^{-1} mol l^{-1}	
Time range:		10 to 1210 s with 30 s intervals	
Noise standard deviation [a]:		0.030	
Composition of solutions (relative concentration)			
No.	Species 1	Species 2	
1 [b]	**1.00**	**1**	
2	1.25	1	
3	1.50	1	
4	1.75	1	
5	2.00	1	
6	1.00	0	
Series II:			
Width of peaks:		20 arbitrary units	
Wavelength range:		1 to 100 with intervals of 1 arbitrary unit	
Position of peaks:		40/50/60 for species 1/2/3/, respectively	
Rate constants:		$k_1 = 4 \times 10^{-3}$ s^{-1}	
		$k_2 = 2 \times 10^{-3}$ s^{-1}	
		$k_3 = 0.15$ s^{-1} mol l^{-1}	
Time range:		10 to 1210 s with 30 s interval	
Noise standard deviation [a]:		0.030	
Composition of solutions (relative concentration)			
No.	Species 1	Species 2	Species 3
1 [b]	**1.00**	**0.5**	**1**
2	1.25	0.5	1
3	1.50	0.5	1
4	1.75	0.5	1
5	2.00	0.5	1
6	1.00	0	0

[a] The noise standard deviation is the value given multiplied by the maximum absorbance value in each data matrix.
[b] Mixture No. 1 is used as the unknown sample. The errors of the estimated concentrations are given in Table 11.

the components was supposed to follow a second-order kinetic law, and the other (or the other two components) was assumed to obey the first-order kinetic law. The responses would be expressed by Eqs. (2) and (9), respectively. The parameters used in this simulation are shown in Table 7. Only the first-order components were considered as the analytes. In order to obtain trilinear data arrays, the standard addition method was used to construct a series of mixtures with increasing analyte concentrations. The solution of the isolated analyte, or one of the mixtures after a standard addition of the analyte, was used as the calibration sample for GRAM, and three of the mixtures obtained by standard addition were used as the multiple calibration samples with TLD. The first mixture (the original sample) was regarded as the unknown sample.

6. Results and discussion

6.1. Simulated data without noise

For the noise-free data (Table 3), the estimated concentrations in all cases coincided with that used in the simulation within the round-off error range, and the spectra and the kinetic curves were almost exactly the same as those initially assumed. There was no difference between GRAM and TLD. This indicated that these methods were correctly implemented and also hinted that, at least in the absence of noise, the accuracy of the estimates of the concentrations and physical profiles obtained by GRAM and TLD was not affected by the collinearity among spectra and kinetic curves of the components.

6.2. Two-component mixtures that follow independent first-order reactions with noise

The relative errors of the estimated concentrations at the different noise levels and various degrees of spectral and kinetic overlap assumed in Table 4, are shown in Table 8. The upper part of Table 8 (corresponding to cases 1 to 5 in Table 4) lists the results of a two-component mixture (No. 10 in Table 4) at different noise levels. The first six columns are the results obtained with GRAM, where a single component solution was used for calibration. Columns seven and eight are the results given by TLD, where all the three single component solutions were used as calibration samples, and the last two columns list the results obtained with TLD by using nine mixtures as

Table 8
Simulated mixtures of two components that follow first-order kinetics: relative error of the estimated concentrations (in percentage) at different noise levels and various degrees of spectral and kinetic collinearities

Case No.	GRAM						TLD			
	Calibration sample No. [a]						Calibration sample Nos. [a]			
	11 (from 11 to 13, component 1)	12	13	14 (from 14 to 16, component 2)	15	16	11–13 (comp. 1)	14–16 (comp. 2)	1–9 (comp. 1)	1–9 (comp. 2)
Series I (different noise level)										
1	−0.45 (I) [b]	−0.11 (I)	0.38 (I)	0.18 (I)	0.015 (I)	0.039 (I)	−0.087 (I)	−0.67 (II)	−0.30 (II)	0.13 (II)
2	−0.66 (I)	−0.63 (I)	−0.44 (I)	1.1(I)	1.0 (I)	1.1 (I)	−0.53 (I)	−0.34 (III)	−0.11(II)	−0.022(II)
3	0.41 (I)	−0.44 (I)	−0.66 (I)	3.0 (I)	2.7 (I)	3.3 (I)	−1.0 (I)	2.6 (I)	−0.50 (II)	−0.67 (II)
4	−3.4 (II)	−3.3 (II)	−2.2 (I)	5.6 (I)	5.2 (I)	5.6 (I)	−4.1 (II)	5.0 (II)	3.5 (II)	−2.2 (II)
5	−7.6 (II)	−7.4 (II)	−4.9 (II)	12 (I)	11 (II)	12 (II)	−9.5 (II)	12 (II)	−6.1 (III)	21 (III)
Series II (different spectral and kinetic overlap)										
6	0.41 (I)	−0.44 (I)	−0.66 (I)	3.0 (I)	2.7 (I)	3.3 (I)	−1.0 (I)	2.6 (I)	−0.50 (II)	−0.67 (II)
7	−2.9 (I)	−2.8 (I)	−1.8 (I)	4.3 (I)	4.8 (I)	4.4 (I)	−3.3 (II)	3.7 (I)	2.3 (II)	−1.5 (II)
8	−4.9 (II)	−4.5 (I)	−2.4 (I)	6.0 (I)	5.9 (I)	6.3 (I)	−5.4 (II)	5.9 (I)	−2.9 (II)	7.8 (II)
9	−3.4 (I)	−3.3 (I)	−2.2 (I)	5.6 (I)	5.2 (I)	5.6 (I)	−0.12 (II)	5.8 (I)	7.3 (II)	−4.9 (II)
10	−1.4 (II)	−16 (II)	5.8 (I)	6.1 (I)	6.5 (I)	14 (I)	−4.5 (II)	9.8 (II)	3.4 (II)	2.7 (II)

[a] The composition of the mixtures was given in Table 4.
[b] The values of the linear correlation coefficients between the calculated and the assumed spectra and kinetic curves are indicated between parentheses: I, both of them were $r > 0.999$; II, the smaller one was $0.99 < r < 0.999$; III, at least one was $r < 0.99$.

calibration samples. From the upper part of the table, the accuracy of the estimated concentrations and physical profiles in both orders of the instrument degraded slightly as the noise level increased, however satisfactory qualitative and quantitative results were obtained for the binary mixtures at all the noise levels tried with both GRAM and TLD. There was no significant difference when the single component solution with various concentrations was used as the calibration sample for GRAM. Also, the performance of GRAM and TLD was almost the same.

The results for the same two-component mixtures with increasing spectral and kinetic overlap are given in the lower part of Table 8. With the moderate noise level adopted, both GRAM and TLD accurately resolved the mixtures with quite large overlap in both orders of the instrument. Similarly to cases 1 to 5, no significant improvement of TLD over GRAM was observed in spite of the larger number of standards used in the former. Therefore, under the condition of ideal bilinear data structure with random noise used in the simulation, a single standard sample is enough in GRAM calibration, and it may be more difficult to retain the trilinearity when multiple samples are used as both the collinearity between physical profiles and the noise level increased.

Table 9 shows the results obtained for the three-component mixtures generated according to the conditions of Table 5. The results obtained with GRAM when one of the single component solutions was used for calibration are listed in the first three columns of Table 9. Calibration with the other single component solutions gave rise to very similar results. The results obtained with TLD calibrated with three single component solutions, and with the nine mixtures, are shown in the successive columns of Table 9. For the three components, the physical profiles were estimated with almost the same accuracy, but the error of the estimated concentration of the second component was higher than that of the other two. Probably, the second component underwent the largest collinearity.

Thus, GRAM and TLD provided acceptable results for the three-component mixtures tried. However, the use of GRAM and TLD on kinetic systems with more components may yield very bad results. Unlike the spectra, kinetic curves exhibit a relatively monotonous shape and do not show much variation for components with quite different rate constants, thus the collinearity in the kinetic aspect would increase rapidly with the number of components. For this three-component system, the ratios of rate constants were 2 and 1.5 for the 1/2 and 2/3 component pairs, respectively. However, the condition

Table 9
Simulated mixtures of three components that follow first order reactions: relative error of the estimated concentrations (in percentages)

Case No.	GRAM			TLD					
	Calibration sample No. [a]			Calibration sample Nos. [a]					
	14 (comp. 1)	17 (comp. 2)	20 (comp. 3)	14–16 (comp. 1)	17–19 (comp. 2)	20–22 (comp. 3)	1–9 (comp. 1)	1–9 (comp. 2)	1–9 (comp. 3)
1	2.1 (I) [b]	8.8 (I)	6.7 (I)	−2.6 (I)	11 (I)	1.3 (III)			
2	1.2 (I)	21 (I)	5.9 (I)	2.3 (I)	23 (I)	1.9 (III)			
3	2.2 (I)	21 (I)	5.1 (I)	7.0 (II)	23 (I)	2.3 (III)			
4	6.5 (I)	9.9 (I)	8.2 (I)	7.4 (I)	10 (I)	6.2 (III)			
5	2.7 (I)	11 (I)	4.9 (I)	9.9 (I)	13 (I)	1.1 (III)			
6	2.1 (I)	12 (I)	8.0 (I)	8.5 (I)	11 (I)	11 (III)			
7	6.1 (I)	4.9 (I)	5.9 (I)	6.0 (I)	5.8 (I)	1.1 (III)			
8	1.5 (I)	0.1 (I)	9.9 (I)	8.8 (I)	7.1 (I)	6.3 (III)			
9	2.2 (I)	10 (III)	28 (I)	2.6 (I)	60 (III)	16 (III)			
10	1.3 (I)	−2.7 (I)	8.5 (I)	5.5 (I)	−1.7 (I)	−1.5 (III)	−2.0 (II)	3.5 (III)	−2.6 (III)
11	3.2 (I)	3.5 (I)	7.5 (I)	10 (I)	4.8 (I)	5.8 (III)	−2.1 (II)	4.6 (III)	−1.7 (III)
12	1.5 (I)	4.5 (I)	11 (I)	2.1 (II)	5.1 (I)	0.68 (III)	−2.3 (II)	2.6 (III)	5.7 (III)
13	2.2 (I)	7.9 (I)	11 (I)	4.6 (II)	7.8 (I)	2.5 (III)	1.5 (II)	−0.47 (III)	2.3 (III)

[a] The composition of the mixtures is given in Table 5.
[b] The roman figures between parentheses have the same meaning as in Table 8.

number of the kinetic curves of these components was 138, which indicated a very strong collinearity among the components. Furthermore, the second component exhibited the strongest collinearity, which agreed with the higher error found. A further increase of the number of components would largely increase the collinearity and the error.

The number of principal components (PCs) used in GRAM and TLD is an important factor. According to Sanchez and Kowalski [13], to overdetermine the number of PCs is better than to underdetermine it. However, in order to avoid a complex solution, the use of a smaller number of PCs than the optimal number is sometimes preferred [5]. With the simulated data sets of above, we have also investigated the influence of the number of PCs. For the two- and three-component mixtures, from a number of PCs equal to the number of intrinsic components (2 or 3) up to 7 PCs have been used to construct the GRAM and TLD models. No obvious influence of the number of PCs on the estimated concentration and physical profiles was found. To increase the number of PCs increased the possibility of occurrence of complex eigen solutions, but most of them had no significant influence on the final results, because the imaginary part could be almost ignored. Furthermore, sometimes it was found that to further increase the number of PCs resulted in the elimination of the complex solutions which appeared with the use of a fewer number of PCs. This hinted that the collinearity may not be the only cause for the outcrop of complex solutions. The determination of the number of PCs will not be a serious problem in the use of GRAM and TLD for kinetic data treatment, since usually a limited number of components is to be found. The number of PCs is established on the basis of the relative magnitude of the eigenvalues. This will yield a number of PCs not far from the true number of intrinsic components. Then the correlation coefficients between the estimated physical profiles and the 'true' ones will be calculated for several values of the number of PCs, and the one providing the largest correlation will be selected.

There is an important difference between GRAM and TLD. The use of GRAM for qualitative purposes requires the physical profiles of the components to be known, which is not necessary in TLD. When several standards are used for calibration in TLD, the identification of the component can be carried out by calculating the correlation coefficients between the estimated concentration profile and the real pattern of the component in the standards. Then, the compo-

Table 10
Simulated mixtures of two components when one of them undergoes a first-order reaction and the other one two consecutive first-order reactions: relative error of the estimated concentration (in percentages)

Case No.	GRAM		TLD			
	Calibration sample No. [a]		Calibration sample Nos. [a]			
	14 (comp. 1)	17 (comp. 2)	14–16 (comp. 1)	17–19 (comp. 2)	1–9 (comp. 1)	1–9 (comp. 2)
1	1.7 (I) [b]	0.24 (I)	2.8 (II)	−2.4 (III)		
2	1.2 (I)	0.15 (I)	2.0 (II)	0.20 (III)		
3	0.20 (I)	−1.3 (I)	0.51 (II)	7.7 (III)		
4	2.7 (I)	−0.46 (I)	6.0 (III)	−1.5 (III)		
5	0.68 (I)	−0.37 (I)	2.7 (III)	−2.7 (III)		
6	1.9 (I)	1.2 (I)	3.1 (III)	−2.4 (III)		
7	4.2 (I)	−0.65 (I)	9.8 (III)	−0.98 (II)		
8	1.3 (I)	−0.25 (I)	5.1 (III)	−1.5 (III)		
9	0.44 (I)	−1.4 (III)	2.5 (III)	−3.2 (III)		
10	0.52 (I)	−1.2 (I)	1.9 (III)	−3.5 (III)	−2.1 (III)	0.92 (III)
11	0.54 (I)	0.046 (I)	1.1 (II)	−4.2 (III)	−1.5 (III)	−0.86 (III)
12	2.0 (I)	−0.40 (I)	5.2 (III)	−1.7 (III)	0.89 (III)	0.25 (III)
13	1.1 (I)	−0.46 (I)	2.9 (III)	−2.5 (III)	−0.56 (III)	−0.33 (III)

[a] The composition of the mixtures is given in Table 6.
[b] The roman figures between parentheses have the same meaning as in Table 8.

Table 11
Mixtures of components that undergo first-order reactions in the presence of a second-order reaction: relative error of the estimated concentration (in percentages)

Number of components	GRAM		TLD
	Calibration sample No. [a]		Calibration sample Nos. [a]
	6 (comp. 1)	5 (comp. 1)	2–5 (comp. 1)
2	0.12 (I) [b]	−0.56 (I)	−0.71 (II)
3	14 (I)	−11 (I)	−6.0 (I)

[a] The composition of the mixtures is given in Table 7.
[b] The roman figures between parentheses have the same meaning as in Table 8.

nent can be determined by the interpolation on the linear calibration function constructed with the concentrations of the standards.

6.3. Simulated mixtures when one of the components undergoes two consecutive first-order reactions

The results given in Table 10 are similar to those shown in Table 9, indicating that the actual reaction mechanism is not important, as long as the data follow bilinear or trilinear relationships with respect to the evaluated parameters. For GRAM, only the results obtained by calibration with one of the single component solutions were listed, since calibration with other single component solutions gave rise to very similar results.

6.4. Simulated mixtures in the presence of a second-order kinetic reaction

Table 11 shows the results obtained with mixtures of two and three components that follow first-order reactions in the presence of a second-order reaction. Since the response of the component that undergoes the second-order reaction cannot be modelled by the trilinear model, the determination of the other components following first-order reactions should be performed by the standard addition method with a fixed background that includes the second-order reacting component. This would preserve the trilinearity in the resultant third-order tensor. In both series of mixtures listed in Table 7, mixture No. 1 was assumed to be the unknown original sample, and the other mixtures obtained after standard addition were used as the calibration samples with TLD. The calibration sample for GRAM was either a single component solution or a mixture after standard addition. The results

Table 12
Relative errors of the estimated concentrations (in percentages) for the *o*-ABA/ORC mixtures

Exp. No.	GRAM						TLD			
	Calibration sample No. [a]						Calibration sample Nos. [a]			
	14 (from 14 to 16, *o*-ABA)	15	16	17 (from 17 to 19, ORC)	18	19	14–16 (*o*-ABA)	17–19 (ORC)	1–9 (*o*-ABA)	1–9 (ORC)
1	1.7 (I) [b]	−1.2 (I)	−4.3 (I)	−1.3 (III)	0.50 (III)	−7.4 (III)	−0.20 (I)	−8.5 (III)		
2	−1.9 (I)	−2.5 (I)	−4.9 (I)	−7.8 (III)	−7.5 (III)	−3.3 (III)	−2.5 (I)	−1.1 (III)		
3	−0.64 (I)	0.73 (I)	−1.1 (I)	−5.1 (III)	−5.6 (III)	1.3 (III)	0.33 (I)	−8.7 (III)		
4	6.5 (II)	1.1 (I)	−3.8 (I)	−0.48 (III)	−5.0 (III)	0.44 (III)	3.9 (I)	−2.1 (III)		
5	5.6 (II)	2.6 (I)	−6.4 (I)	−6.3 (III)	−4.4 (III)	−1.8 (III)	3.1 (I)	−4.7 (III)		
6	3.6 (I)	4.1 (I)	1.6 (I)	−3.6 (III)	−4.2 (III)	2.6 (III)	5.0 (I)	−1.3 (III)		
7	14 (I)	−4.2 (I)	−0.70 (I)	−4.3 (III)	−2.5 (III)	3.0 (III)	6.3 (I)	−2.8 (III)		
8	6.1 (II)	7.9 (I)	3.9 (I)	2.0 (III)	1.4 (III)	8.7 (III)	5.8 (I)	7.3 (II)		
9	4.2 (I)	5.4 (I)	2.2 (I)	1.0 (III)	0.42 (III)	7.8 (III)	2.6 (I)	6.1 (III)		
10	6.5 (II)	3.5 (I)	−0.34 (I)	0.18 (I)	3.6 (III)	2.3 (III)	2.3 (I)	−0.80 (III)	−3.9 (II)	2.9 (III)
11	8.0 (II)	14 (I)	6.2 (I)	−2.3 (I)	−2.9 (III)	4.9 (III)	9.8 (I)	1.5 (III)	3.1 (II)	−0.30 (III)
12	12 (II)	12 (I)	11 (I)	6.5 (I)	5.4 (III)	23 (III)	12 (I)	8.1 (III)	2.5 (III)	11 (III)
13	13 (II)	9.5 (I)	7.4 (I)	−2.9 (I)	−2.7 (III)	5.1 (III)	5.8 (I)	−0.15 (III)	−0.96 (III)	−4.2 (III)

[a] The composition of the mixtures is given in Table 2.
[b] The roman figures between parentheses have the same meaning as in Table 8.

Table 13
Relative errors of the estimated concentrations (in percentages) for the *m*-ABA/*p*-ABA mixtures

Exp. No.	GRAM						TLD			
	Calibration sample No. [a]						Calibration sample Nos. [a]			
	14 (from 14 to 16, *m*-ABA)	15	16	17 (from 17 to 19, *p*-ABA)	18	19	14–16 (*m*-ABA)	17–19 (*p*-ABA)	1–9 (*m*-ABA)	1–9 (*p*-ABA)
1	−2.0 (I) [b]	2.1 (I)	1.5 (I)	4.5 (I)	6.4 (I)	7.4 (I)	8.7 (I)	6.0 (I)		
2	−4.4 (I)	−0.22 (I)	−1.4 (I)	4.0 (I)	5.8 (I)	7.0 (I)	7.5 (I)	6.5 (I)		
3	−5.7 (I)	−1.1 (I)	−2.5 (I)	4.4 (I)	6.5 (I)	7.5 (I)	4.4 (I)	6.4 (I)		
4	1.2 (I)	5.3 (I)	4.3 (I)	2.0 (I)	5.3 (I)	5.5 (I)	0.90 (I)	5.4 (I)		
5	0.26 (I)	2.3 (I)	2.5 (I)	1.6 (I)	3.5 (I)	4.1 (I)	5.3 (I)	4.1 (I)		
6	−0.98 (I)	0.038 (I)	1.1 (I)	1.5 (I)	3.1 (I)	3.9 (I)	2.7 (I)	4.0 (I)		
7	−0.070 (I)	5.4 (I)	−0.13 (I)	−2.7 (I)	−0.98 (I)	−0.46 (I)	1.1 (I)	0.24 (I)		
8	−2.0 (I)	2.8 (I)	−1.9 (I)	−2.8 (I)	−1.3 (I)	−0.52 (I)	1.8 (I)	−0.13 (I)		
9	−0.74 (I)	4.3 (I)	−4.3 (I)	−0.28 (I)	−0.28(I)	7.9 (I)	5.8 (I)	5.3 (I)		
10	−1.2 (I)	5.4 (I)	0.75 (I)	−1.3 (I)	−0.022 (I)	1.9 (I)	1.2 (I)	4.4 (I)	−0.083 (I)	−0.58 (I)
11	−0.33 (I)	2.2 (I)	0.45 (I)	−0.63 (I)	1.6 (I)	−0.050 (I)	0.48 (I)	2.0 (I)	0.97 (I)	−4.60 (I)
12	11 (I)	8.7 (I)	11 (I)	5.1 (I)	7.4 (I)	7.7 (I)	0.92 (I)	8.6 (I)	12 (I)	3.7 (I)
13	1.8 (I)	2.3 (I)	3.7 (I)	0.17 (I)	2.8 (I)	2.9 (I)	−0.42 (I)	2.6 (I)	1.8 (I)	−8.3 (I)

[a] The composition of the mixtures is given in Table 2.
[b] The roman figures between parentheses have the same meaning as in Table 8.

are listed in Table 11. The estimated physical profiles for the two- and three-component mixtures were accurate, but the error in the estimated concentrations was somewhat higher for the latter owing to the stronger collinearity.

6.5. Resolution of binary mixtures

The results obtained with GRAM and TLD for the series of binary mixtures are listed in Tables 12–14. Both the physical profiles and the concentrations were

Table 14
Relative errors of the estimated concentrations (in percentages) for the *o*-ABA/*m*-ABA mixtures

Exp. No.	GRAM						TLD			
	Calibration sample No. [a]						Calibration sample Nos. [a]			
	14 (from 14 to 16, *o*-ABA)	15	16	17 (from 17 to 19, *m*-ABA)	18	19	14–16 (*o*-ABA)	17–19 (*m*-ABA)	1–9 (*o*-ABA)	1–9 (*m*-ABA)
1	1.5 (I) [b]	−0.16 (I)	4.9 (I)	27 (II)	27 (II)	22 (III)	5.8 (I)	21 (III)		
2	−5.8 (I)	−7.0 (I)	−6.5 (I)	34 (II)	34 (II)	18 (III)	−5.4 (I)	16 (III)		
3	−5.0 (I)	−6.5 (I)	−6.5 (I)	45 (II)	46 (II)	22 (III)	−5.5 (I)	20 (III)		
4	6.8 (I)	5.2 (I)	4.2 (I)	22 (II)	22 (I)	18 (III)	6.7 (II)	19 (III)		
5	5.3 (I)	3.6 (I)	2.5 (I)	25 (I)	26 (II)	18 (III)	9.3 (I)	16 (III)		
6	5.5 (I)	3.5 (I)	2.2 (I)	22 (II)	24 (III)	15 (II)	6.6 (I)	11 (III)		
7	26 (I)	39 (I)	23 (I)	10 (I)	4.9 (III)	5.0 (III)	38 (I)	4.7 (III)		
8	21 (I)	26 (I)	17 (I)	15 (II)	7.6 (III)	7.3 (II)	25 (I)	7.1 (III)		
9	19 (I)	20 (I)	15 (I)	26 (III)	17 (III)	15 (II)	20 (I)	15 (III)		
10	13 (I)	11 (I)	9.8 (I)	13 (I)	14 (I)	12 (III)	7.2 (II)	12 (III)	−0.30 (I)	−3.7 (III)
11	22 (I)	20 (I)	14 (I)	9.6 (III)	9.0 (III)	12 (II)	19 (I)	7.8 (III)	3.0 (I)	−0.79 (III)
12	28 (I)	26 (I)	25 (I)	20 (II)	21 (II)	14 (II)	28 (II)	15 (II)	13 (I)	2.5 (III)
13	17 (I)	16 (I)	8.9 (I)	8.0 (III)	7.4 (III)	8.7 (II)	15 (I)	6.0 (III)	−1.4 (I)	−5.0 (III)

[a] The composition of the mixtures is given in Table 2.
[b] The roman figures between parentheses have the same meaning as in Table 8

estimated with quite small errors for the *o*-ABA/ORC and *m*-ABA/*p*-ABA mixtures, thus showing that the 'second-order advantage' can also be exploited using kinetic-spectral data. However, for the *o*-ABA/*m*-ABA mixtures, the error of the estimates of the concentrations was much higher than for the other binary combinations, although the estimates of the physical profiles were still quite satisfactory. This should be attributed to the very large spectral and kinetic overlap of this substrate combination. The number of PCs used in the calculation was 2 or 3, depending on the correlation between the calculated physical profiles and the measured ones.

Acknowledgements

Work supported by the DGICYT of Spain, Project PB93/355. Y.L. Xie is grateful for a postdoctoral grant from the Ministry of Education and Science of Spain.

References

[1] K.S. Booksh and B.R. Kowalski, Anal. Chem., 66 (1994) 782A.
[2] T. Hirschfeld, Science, 230 (1985) 286.
[3] T. Hirschfeld, Anal. Chem., 52 (1980) 297A.
[4] R. Tauler and E. Casassas, Analusis, 20 (1992) 255.
[5] Z.H. Lin, K.S. Booksh, L.W. Burgess and B.R. Kowalski, Anal. Chem., 66 (1994) 2552.
[6] K.S. Booksh, Z.H. Lin, Z.Y. Wang and B.R. Kowalski, Anal. Chem., 66 (1994) 2561.
[7] Y.D. Wang, O.S. Borgen, B.R. Kowalski, M. Gu and F. Turecek, J. Chemom., 7 (1994) 117.
[8] E. Sanchez and B.R. Kowalski, J. Chemom., 2 (1988) 265.
[9] Y.D. Wang, O.S. Borgen and B.R. Kowalski, J. Chemom., 7 (1993) 439.
[10] A.K. Smilde, Y.D. Wang and B.R. Kowalski, J. Chemom., 8 (1994) 21.
[11] E. Sanchez and B.R. Kowalski, Anal. Chem., 58 (1986) 496.
[12] C.J. Appellof and E.R. Davidson, Anal. Chem., 53 (1981) 2053.
[13] E. Sanchez and B.R. Kowalski, J. Chemom., 4 (1990) 29.
[14] C.N. Ho, G.D. Christian and E.R. Davidson, Anal. Chem., 50 (1978) 1108.
[15] A. Lorber, Anal. Chim. Acta, 164 (1984) 293.
[16] A. Lorber, Anal. Chem., 57 (1985) 2395.
[17] N.M. Faber, L.M.C. Buydens and G. Kateman, J. Chemom., 8 (1994) 147.
[18] B.E. Wilson, E. Sanchez and B.R. Kowalski, J. Chemom., 3 (1989) 493.
[19] K. Booksh and B.R. Kowalski, J. Chemom., 8 (1994) 45.
[20] B.C. Mitchell and D.S. Burdick, Chemom. Intell. Lab. Syst., 20 (1993) 149.
[21] S.S. Li, C. Hamilton and P.J. Gemperline, Anal. Chem., 64 (1992) 599.
[22] K.S. Booksh and B.R. Kowalski, J. Chemom., 8 (1994) 287.
[23] E. Sanchez, L.S. Ramos and B.R. Kowalski, J. Chromatogr., 385 (1987) 151.
[24] L.S. Ramos, E. Sanchez and B.R. Kowalski, J. Chromatogr., 385 (1987) 165.
[25] S.S. Li and P.J. Gemperline, J. Chemom., 7 (1993) 77.
[26] B.M. Quencer and S.R. Crouch, Analyst, 118 (1993) 695.
[27] B.M. Quencer and S.R. Crouch, Anal. Chem., 66 (1994) 458.
[28] Y.L. Xie, J.J. Baeza-Baeza and G. Ramis-Ramos, Anal. Chim. Acta, in press.
[29] M. Blanco, J. Coello, H. Iturriaga, S. Maspoch, J. Riba and E. Rovira, Talanta, 40 (1993) 261.
[30] J. Havel, F. Jiménez, R.D. Bautista and J.J. Arias-León, Analyst, 118 (1993) 1355.
[31] Y.L. Xie, J.J. Baeza-Baeza and G. Ramis-Ramos, Chemom. Intell. Lab. Syst., 27 (1995) 211.
[32] A. Cladera, E. Gómez, J.M. Estela and V. Cerdà, Anal. Chem., 65 (1993) 707.
[33] G. Ramis-Ramos, J.S. Esteve-Romero and M.C. García Alvarez-Coque, Anal. Chim. Acta, 223 (1989) 327.
[34] J.S. Esteve-Romero, M.C. García Alvarez-Coque and G. Ramis-Ramos, Talanta, 38 (1991) 1285.
[35] K.A. Connors, Chemical Kinetics – The Study of Reaction Rates in Solution, VCH, 1990.
[36] L. Norgaard and C. Ridder, Chemom. Intell. Lab. Syst., 23 (1994) 107.
[37] S. Wold, P. Geladi, K. Esbensen and J. Öhman, J. Chemom., 1 (1987) 41.
[38] Y.L. Xie, J.H. Wang, Y.Z. Liang and R.Q. Yu, Anal. Chim. Acta, 281 (1993) 207.
[39] G.H. Golub and C.F. van Loan, Matrix Computations, The Johns Hopkins University Press, Baltimore, MD, 1989, Chap. 7.